Yrast spectroscopy in the neutron-deficient nucleus ^{169}Os

D. T. Joss,[1,2] J. Simpson,[1] R. D. Page,[3] S. L. King,[3] N. Amzal,[3] D. E. Appelbe,[1] T. Bäck,[4] M. A. Bentley,[2] B. Cederwall,[4] J. F. C. Cocks,[5] D. M. Cullen,[3,*] P. T. Greenlees,[3,†] K. Helariutta,[5] P. M. Jones,[5] R. Julin,[5] S. Juutinen,[5] H. Kankaanpää,[5] A. Keenan,[3,†] H. Kettunen,[5] P. Kuusiniemi,[5] M. Leino,[5] M. Muikku,[5] A. Savelius,[5] J. Uusitalo,[5] D. D. Warner,[1] S. J. Williams,[2] and R. Wyss[4]

[1]*CLRC, Daresbury Laboratory, Daresbury, Warrington WA4 4AD, United Kingdom*

[2]*School of Chemistry and Physics, Keele University, Keele, Staffordshire ST5 5BG, United Kingdom*

[3]*Oliver Lodge Laboratory, University of Liverpool, Liverpool L69 7ZE, United Kingdom*

[4]*Department of Physics, Royal Institute of Technology, SE-106 91 Stockholm, Sweden*

[5]*Department of Physics, University of Jyväskylä, P.O. Box 35, FIN-40351 Jyväskylä, Finland*

(Received 8 July 2002; published 27 November 2002)

Excited states in the neutron-deficient isotope ^{169}Os have been identified for the first time in an experiment using the Jurosphere γ-ray spectrometer in conjunction with the Ritu gas-filled recoil separator. The problems associated with identifying neutron-deficient isotopes produced with low fusion cross sections against a high background of competing channels, including fission, have been overcome by using the recoil-decay tagging technique. The band structures observed in ^{169}Os are interpreted in the context of the systematics of neighboring nuclei and the predictions of cranked Woods-Saxon calculations. The systematics of the second $(i_{13/2})^2$ neutron alignment in this region are discussed.

DOI: 10.1103/PhysRevC.66.054311 PACS number(s): 29.30.Kv, 21.10.Re, 23.20.Lv, 27.70.+q

I. INTRODUCTION

The neutron-deficient osmium isotopes with $N<96$ occupy a transitional region with respect to evolving nuclear shapes. Isotopes near the mid-shell at $N=104$ are known to exhibit shape coexistence due to the interaction between a weakly deformed ground-state band and a deformed-prolate band that is associated with proton excitations across the $Z=82$ shell closure [1]. A noted example of shape coexistence in this mass region is manifested by the pronounced perturbation of the energy of the yrast states in ^{172}Os at spin $\approx 6\hbar$ [2], which has been successfully interpreted in terms of phenomenological band mixing calculations [3–5]. In the more neutron-deficient isotopes ^{171}Os [6], ^{170}Os [3], and ^{168}Os [7], band mixing calculations suggest that the deformed-prolate intruder band lies at increasingly higher excitation energies relative to the ground-state band as the neutron number decreases towards the $N=82$ shell gap. Yrast energy level systematics for the even-N osmium isotopes suggest the lowering of the average deformation as the neutron number recedes from the neutron mid-shell value [7]. In addition, mixing with vibrational structures becomes more important as observed in studies of non-yrast states in the neutron-deficient platinum [8,9], osmium [10], and tungsten [11] isotopes. It is clearly valuable to deduce the level structure of odd-mass neutron-deficient isotopes in order to identify the core polarizing orbitals at the Fermi surface and to provide stringent constraints on theoretical models describing this transitional region.

Although significant advances have been made in understanding nuclear structure in this region, in-beam spectroscopy of the $N<94$ osmium isotopes is a challenging experimental task. This is mainly because the fusion cross sections for the channels of interest decrease rapidly further from the valley of stability and it becomes difficult to separate the desired channels from a large background of competing channels including fission. This problem has been overcome by the application of the highly selective tagging technique known as recoil-decay tagging (RDT) [12,13]. This paper reports the first observation of excited states in the odd-mass nucleus ^{169}Os, made possible by the use of the recoil-decay tagging technique. The yrast sequence has been established up to $E_x=3625$ keV and other non-yrast structures have been observed. The bands are discussed in terms of quasiparticle alignments in the context of Woods-Saxon cranking calculations.

II. EXPERIMENT

Excited states in ^{169}Os have been identified for the first time in an experiment performed at the Accelerator Laboratory of the University of Jyväskylä using the K130 cyclotron. The ^{112}Sn(^{60}Ni,$x\alpha ypzn$) reaction at a beam energy of 265 MeV was used to populate excited states in a variety of nuclei, with ^{169}Os being populated via the $2pn$ evaporation channel. The ^{112}Sn target comprised two stacked self-supporting foils, each of nominal thickness 500 μg/cm^2. Prompt γ rays were detected at the target position by the Jurosphere γ-ray spectrometer consisting of 13 Eurogam [14] and 12 Tessa-type [15] escape-suppressed Ge detectors. For this experiment the Eurogam Ge detectors were positioned at backward angles to the beam direction (five at 157.6° and eight at 133.6°), while the Tessa-type Ge detectors were placed almost perpendicular to the beam direction (five at 79° and five at 101°). Two additional Tessa-type Ge detectors were positioned inside Eurogam suppression

*Present address: Schuster Laboratory, University of Manchester, Manchester M13 9PL, UK.

†Present address: Department of Physics, University of Jyväskylä, PO Box 35, FIN-40351, Jyväskylä, Finland.

shields at 133.6°. The total photopeak efficiency of the Jurosphere spectrometer was measured to be ≈1.5% at 1.3 MeV. The Ritu gas-filled recoil separator [16, 17] was used to separate fusion-evaporation residues from fission products and the scattered beam and to transport the desired fusion products to a silicon strip detector located at the focal plane. The silicon detector was position sensitive in the vertical direction and composed of sixteen 5 mm wide strips, with overall active dimensions of 80 mm×35 mm.

III. RESULTS

A. Identification of ^{169}Os

Recoil-decay tagging experiments correlate prompt γ rays detected at the target position with the subsequent α (or proton) decays of recoils implanted in a silicon strip detector at the focal plane of a recoil separator. The RDT technique establishes high-confidence correlations under the optimum conditions of short radioactive decay half lives and high α (or proton) branching ratios. Neutron-deficient nuclei formed following fusion-evaporation reactions decay via several exit channels to many residual nuclei that have different characteristic decay half lives and branching ratios.

Typically, in an RDT experiment the recoil counting rate is optimized according to the general rule

$$\text{rate} < \frac{N_{pixels}}{3t_{1/2}}, \tag{1}$$

where N_{pixels} is the number of pixels and $t_{1/2}$ is the decay half life of the nuclide of interest. The reaction reported in this paper was optimized with respect to the α-decay properties of ^{170}Pt ($t_{1/2}=14.7\pm5$ ms, $b_\alpha=100\%$) [18], which was populated via the $2n$ exit channel with a cross section of $\sigma\approx30$ μb [19]. The experimental cross section for ^{169}Os was estimated from measured α-particle yields to be $\sigma\approx700$ μb, however the α-decay half life is much longer at $t_{1/2}=3.6\pm0.2$ s, and the branching ratio is significantly lower at $b_\alpha=11\pm1\%$ [20]. The recoil implantation rate in the silicon strip detector for this experiment was typically 2 kHz, which places an upper half life limit for high-confidence correlations at $t_{1/2}\approx30$ ms. In circumstances such as those in the present case, where correlations are performed for non-optimal evaporation channels with long half lives and high recoil implantation rates, the probability of false correlations due to multiple hits in the same pixel within a designated correlation time is greatly increased. Hence, the decay properties of ^{169}Os preclude identification using a straightforward application of the recoil-decay tagging technique under these experimental conditions.

In order to assign the previously unidentified γ rays observed in this experiment to ^{169}Os, a variation of the RDT method that has proved successful in correlating γ-ray transitions with the α decays of non-optimal channels has been applied (see Ref. [7] for further details). Following the detection of an α particle at the focal plane, the data were sorted with a search time of 2 s in order to find an associated ''parent'' recoil in the same pixel. Upon the first recoil-α correlation the γ rays in coincidence with the tagged recoil were incremented with the α-particle energy into an E_γ-E_α correlation matrix. Although the long search time used in this analysis produced a large background of random correlations, selecting specific γ-ray transitions in the E_γ-E_α correlation matrix still allowed the associated α decay(s) to be identified when a fraction of the total α projection from the correlation matrix is subtracted. Figures 1(a) and 1(b) show part of the E_α axis of the correlation matrix close to the characteristic α decays of ^{169}Os ($E_\alpha=5.576$ MeV, $t_{1/2}=3.6\pm0.2$ s, $b_\alpha=11\pm1\%$) and ^{170}Os ($E_\alpha=5.407$ MeV, $t_{1/2}=9\pm1$ s, $b_\alpha=8.6\pm0.6\%$), respectively [20]. The remaining panels of the figure [Figs. 1(c)–1(f)] display the α-particle spectra formed by demanding coincidences with specific γ rays. Coincidences with the 287 keV and 463 keV transitions in ^{170}Os [3] populated via the $2p$ channel are successfully

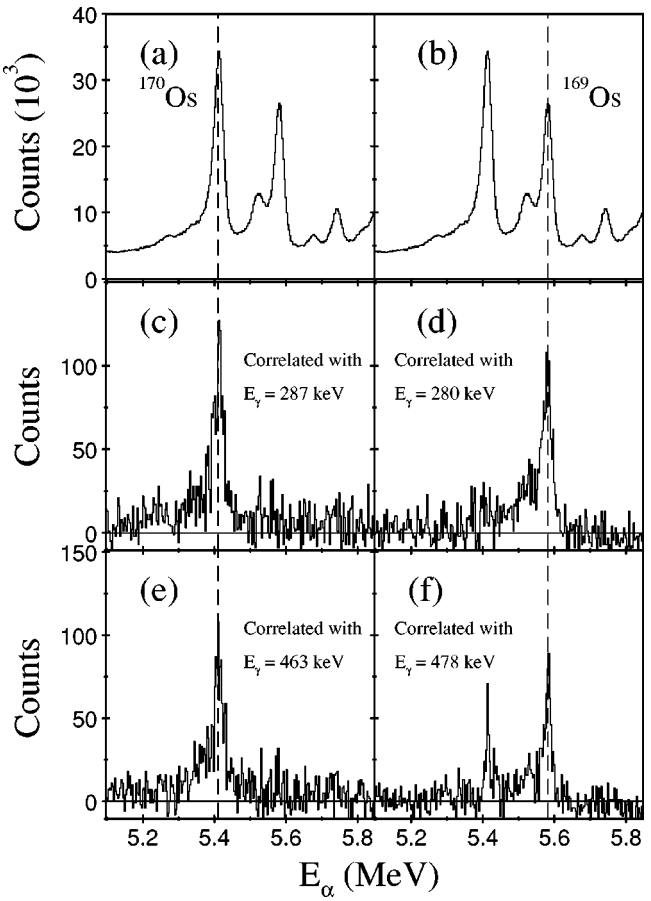

FIG. 1. Alpha-particle energy spectra obtained from an E_γ-E_α matrix. A region of the total projection of the α-particle spectrum expanded around the α peaks of ^{170}Os ($E_\alpha=5.407$ MeV) and ^{169}Os ($E_\alpha=5.576$ MeV), respectively, are shown in (a) and duplicated in (b) to allow comparisons with other spectra. Background subtracted α-particle spectra in coincidence with the 287 keV and 463 keV transitions belonging to ^{170}Os (Ref. [3]) are shown in (c) and (e), respectively. Similar spectra correlated with the 280 keV and 478 keV low-spin transitions identified in this analysis to belong to ^{169}Os are shown in (d) and (f), respectively. The 478 keV transition is a doublet appearing in the yrast sequences of both ^{169}Os and ^{170}Os resulting in a successful correlation with both α-decay lines.

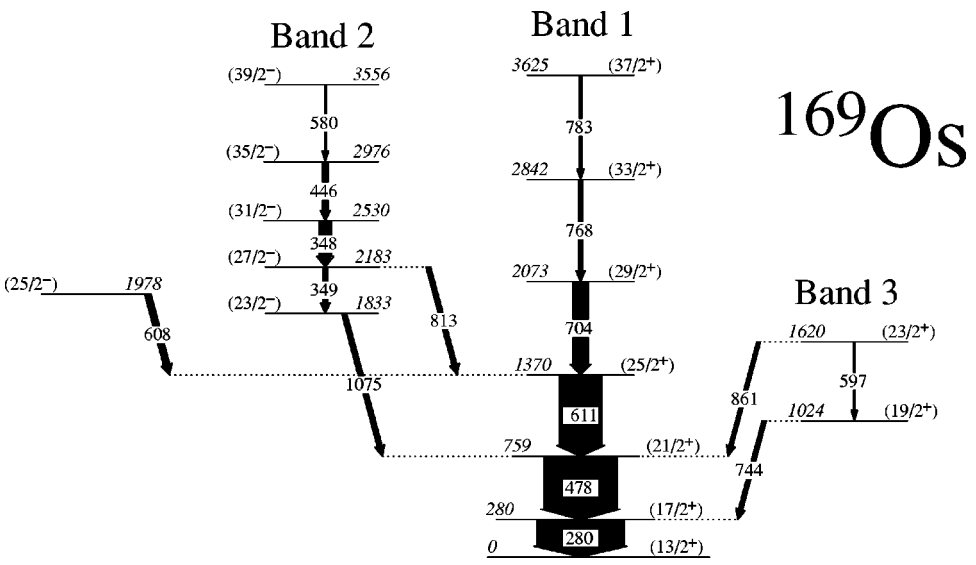

FIG. 2. Level scheme deduced for ^{169}Os from this work. The transition and level excitation energies are given in keV to a precision of 1 keV. The relative intensities are proportional to the widths of the arrows. Tentative spin and parity assignments are shown in parentheses.

correlated with the 5.407 MeV characteristic ^{170}Os α-decay line in Figs. 1(c) and 1(e), respectively. Figures 1(d) and 1(f) show that the 5.576 MeV α decay of ^{169}Os [20] is correlated with the 280 keV and 478 keV γ rays, respectively. It is interesting to note that the 478 keV transition is present in the yrast sequences of both ^{169}Os (see Fig. 2) and ^{170}Os and consequently is correlated with both α-decay lines in Fig. 1(f). This technique establishes that the 280 keV and 478 keV γ-ray transitions belong to ^{169}Os.

B. Recoil-$\gamma\gamma$ coincidence analysis

Gamma-ray events in coincidence with recoils implanted at the focal plane detector were sorted into an $E_{\gamma 1}$-$E_{\gamma 2}$ coincidence matrix. A total of 2.6×10^6 recoil-$\gamma\gamma$ events were collected during this 78 h experiment. The matrix was analyzed using the ESCL8R graphical analysis software package [21] and the resulting level scheme for ^{169}Os is displayed in Fig. 2. A meaningful angular correlation analysis has not been possible due to insufficient statistics. Spin and parity assignments are based on considerations of likely quasiparticle configurations and by comparison with similar structures in neighboring nuclei. Band 1 is assumed to be a collective band based on the $\nu i_{13/2}$ orbital as is the case in the heavier osmium isotopes ^{171}Os [6] and ^{173}Os [22] and neighboring nuclei. All excitation energies are quoted relative to the assumed $(13/2^+)$ band-head state of band 1.

Band 1 consists of six γ-ray transitions and reaches an excitation energy $E_x=3625$ keV and spin (37/2). Figures 3(a) and 3(b) show spectra of band 1 obtained by demanding coincidences with the 280 keV transition (assigned to ^{169}Os in the RDT analysis) and the 768 keV transition. In addition to the band 1 transitions and characteristic osmium x rays, a number of discrete γ-ray transitions belonging to other non-yrast structures can be seen in Fig. 3(a).

The dominant intensity at high spins ($I>25/2$) lies in a second band (labeled band 2 in Fig. 2) that comprises four transitions, which extends to $E_x=3556$ keV. Figure 3(c) shows γ rays in band 2 formed by demanding coincidences with the 349 keV transition. The first two transitions of band 2 form a self-coincident doublet with E_γ around 348.5 keV. The correct ordering of these two transitions is confirmed by the observation of 813 keV and 1075 keV transitions which are observed to decay to band 1 from the $(27/2^-)$ and $(23/2^-)$ states in band 2, respectively. Figure 3(d) shows γ rays in coincidence with the 611 keV transition indicating the decay from band 2 through the 813 keV transition. There is some evidence in these data for other non-yrast structures. Three γ-ray transitions at 744, 861, and 608 keV have been observed to feed into the $(17/2^+)$, $(21/2^+)$, and $(25/2^+)$ states in band 1, respectively. Coincidence relationships suggest that the 744 keV and 861 keV transitions are probably associated with the decay from the same non-yrast band (band 3) by the presence of a weak 597 keV γ ray.

IV. DISCUSSION

The structure of the bands in ^{169}Os are interpreted in this work in terms of quasiparticle configurations within the framework of Woods-Saxon cranking calculations [23]. Quasiparticle Routhians, e', calculated for ^{169}Os are displayed in Fig. 4(a). The labeling convention for quasiparticle Routhians is given in the caption of Fig. 4. In these calculations the pairing strength is modeled with a frequency dependent modification, so that the pairing is gradually reduced to 50% of the zero frequency value at 0.7 MeV/$\hbar$. The deformation parameters ($\beta_2=0.171$, $\beta_4=-0.0023$, $\gamma=4.42°$) used in the cranking calculations are the average values predicted from total Routhian surface calculations for the (parity π, signature α) = (+,+1/2) quasineutron configuration in ^{169}Os. A total Routhian surface calculated at zero frequency for this configuration is plotted in Fig. 4(b). The potential energy surface exhibits a γ-soft minimum centered about small positive γ deformations which is consistent with the interpretation of the results published for ^{171}Os [6] and the predicted influence of the $\nu i_{13/2}$ orbitals on the average deformation [24]. The negative-parity high-Ω orbitals originating from the $\pi h_{11/2}$ sub-shell are the lowest energy proton levels. However, the $h_{11/2}$ quasiproton alignments are predicted to occur at $\omega_{A_pB_p}\approx0.45$ MeV/$\hbar$ and are therefore not

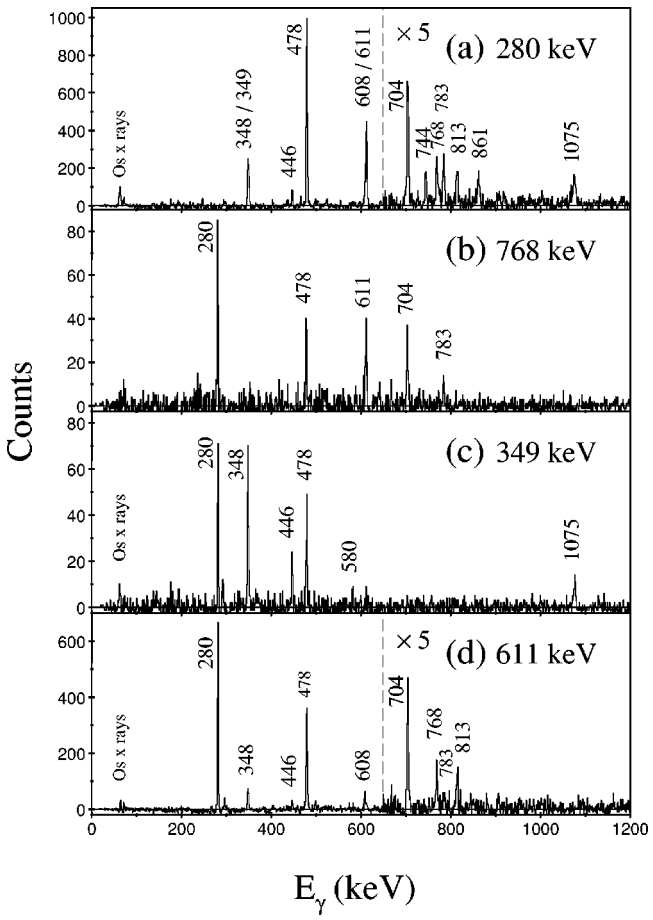

FIG. 3. Examples of γ-ray coincidence spectra generated from a recoil gated $E_{\gamma 1}$-$E_{\gamma 2}$ coincidence matrix with transition energies assigned to ^{169}Os given in keV: (a) spectrum in coincidence with the 280 keV transition; (b) spectrum in coincidence with the 768 keV transition showing γ rays in band 1; (c) spectrum in coincidence with the 349 keV γ ray showing transitions in band 2; (d) spectrum in coincidence with the 611 keV transition showing the decay of band 2 through the 813 keV transition.

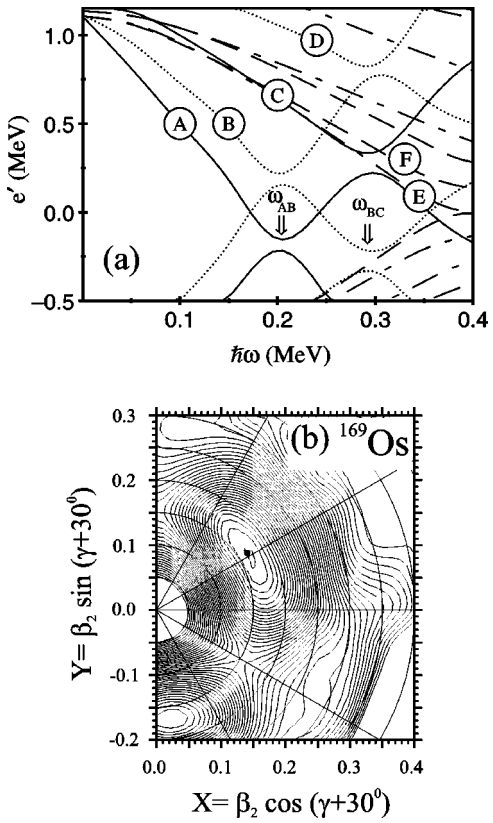

FIG. 4. (a) Cranked Woods-Saxon quasineutron Routhian diagram for ^{169}Os with $\beta_2=0.171$, $\beta_4=-0.0023$, and $\gamma=4.42°$. The quasiparticles are labeled using the standard convention, namely (parity, signature)$=(\pi,\alpha)_n$. $A=(+,+1/2)_1$, $B=(+,-1/2)_1$, $C=(+,+1/2)_2$, $D=(+,-1/2)_2$, $E=(-,+1/2)_1$, and $F=(-,-1/2)_1$. The predicted frequency of the first AB and second BC $(i_{13/2})^2$ quasineutron alignments is indicated. (b) Total Routhian surface calculated for the $(+,+1/2)$ configuration in ^{169}Os at zero frequency. The energy difference between contour lines is 100 keV.

expected to influence the yrast structures significantly in the present experiment.

To facilitate the discussion of the underlying nuclear configurations, the experimental data are presented in terms of the alignment, i_x, as a function of rotational frequency. A rotational reference with a variable moment of inertia defined by the parameters $\mathcal{J}_0=6\ \hbar^2\mathrm{MeV}^{-1}$ and $\mathcal{J}_1=112\ \hbar^4\mathrm{MeV}^{-3}$ has been subtracted from the experimental data according the Harris formula [25]. These parameters were chosen to give a roughly constant alignment for the low-spin states of band 1 in ^{169}Os. The experimental alignments for bands in ^{169}Os are compared with the alignment properties of the neighboring osmium isotopes ^{168,170}Os [3,7] and ^{171}Os [6] in Figs. 5(a) and 5(b), respectively. Band 1 in ^{169}Os, assumed to be the $\nu i_{13/2}$ configuration in Sec. III B, carries an alignment of $7.0\hbar$ at $\omega=0.25$ MeV/$\hbar$, and so has the same nominal alignment as the one quasineutron $(+,+1/2)$ configuration A in ^{171}Os. This assumption is confirmed by the quasiparticle Routhians, Fig. 4(a), which predict that the $(+,+1/2)$ A quasineutron, based on the lowest energy $\nu i_{13/2}$ orbital, is yrast at non-zero rotational frequency with an alignment $(i_x=\mathrm{d}e'/\mathrm{d}\omega)$ of $6.3\ \hbar$ at $\omega=0.1$ MeV/$\hbar$.

Figure 5 shows a gain in alignment in band 1 at $\omega\approx0.4$ MeV/$\hbar$. The alignment of the first pair of $\nu(i_{13/2})$ quasineutrons AB at ≈0.2 MeV/$\hbar$ is blocked in band 1. Therefore, the first alignment is expected to be the second $\nu(i_{13/2})^2$ BC quasineutron alignment, which is predicted to occur at ≈0.3 MeV/$\hbar$. Therefore, the alignment gain observed is interpreted as the onset of the BC crossing. Although the BC crossing frequency cannot be determined from these data, some information about the likely character of this alignment can be inferred from systematic comparisons with neighboring odd-A nuclei. Figures 6(a) and 6(b) show the alignment, i_x, for ^{169}Os and the heavier osmium isotopes and the $N=93$ isotones, respectively. Figure 6(a) shows that ^{173}Os [22] upbends at the BC alignment whereas ^{171}Os [6] backbends suggesting that the interaction strength of the BC crossing becomes weaker with decreasing neutron number. Figure 6(b) shows that the interaction strength at the BC crossing for the $N=93$ isotones becomes much weaker with increasing proton number. If ^{169}Os follows these trends,

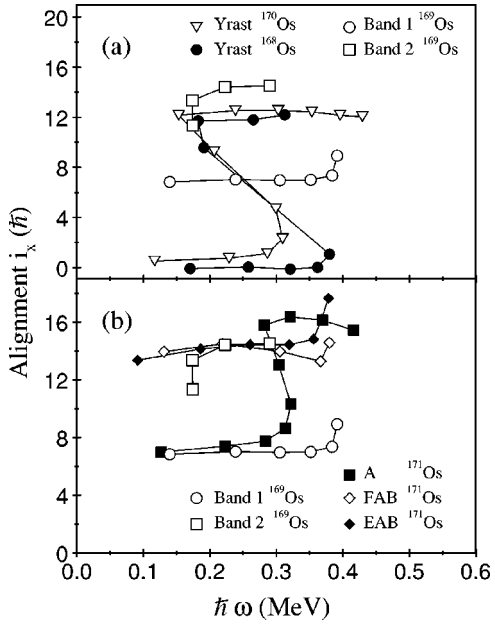

FIG. 5. Experimental alignments i_x as a function of rotational frequency $\hbar\omega$ for (a) yrast bands in ^{168}Os [7], ^{169}Os and ^{170}Os (Ref. [3]) and band 2 in ^{169}Os; (b) the one (A) and three (EAB/FAB) quasiparticle bands in ^{169}Os and ^{171}Os. A rotational reference defined by the parameters $\mathcal{J}_0=6\ \hbar^2\mathrm{MeV}^{-1}$ and $\mathcal{J}_1=112\ \hbar^4\mathrm{MeV}^{-3}$ has been subtracted from each band.

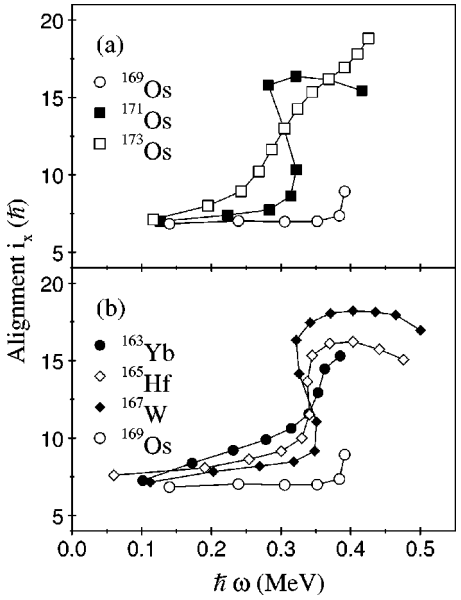

FIG. 6. Experimental alignments i_x as a function of rotational frequency $\hbar\omega$ for (a) yrast bands in ^{169}Os, ^{171}Os (Ref. [6]), and ^{173}Os (Ref. [22]) (b) the yrast band in ^{169}Os and those of the neighboring $N=93$ isotones ^{163}Yb (Ref. [27]), ^{165}Hf (Ref. [29]), and ^{167}W (Ref. [28]). A rotational reference defined by the parameters $\mathcal{J}_0=6\hbar^2\ \mathrm{MeV}^{-1}$ and $\mathcal{J}_1=112\hbar^4\ \mathrm{MeV}^{-3}$ has been subtracted from each band.

a sharp backbend [similar to that observed in the yrast band of ^{168}Os, see Fig. 5(a)], indicative of a weak interaction at the BC alignment, is expected.

Band 2 in ^{169}Os carries an alignment of $14.4\hbar$ at $\omega=0.25$ MeV/$\hbar$. Inspection of Fig. 5(a) shows that the alignment of band 2 is larger than the value determined for the two quasineutron $(\nu i_{13/2})^2$ AB configuration in ^{168}Os and ^{170}Os ($i_x\approx 12\hbar$) suggesting a three quasiparticle configuration. Band 2 in ^{169}Os carries roughly the same alignment between $\omega=0.2$–0.4 MeV/$\hbar$ as the three quasineutron configurations EAB and FAB in ^{171}Os [6]. The experimental alignment is in good agreement with cranking calculations, which predict $i_x\approx 14.5\hbar$ for the EAB and FAB configurations. Hence, band 2 is assigned to be a three quasiparticle configuration (either EAB or FAB) arising from coupling the aligned $(i_{13/2})^2$ quasineutron pair (AB) to one of the available negative-parity quasineutrons originating from the $(f_{7/2}h_{9/2})$ subshell (E or F). Furthermore, band 2 exhibits a drop in alignment at $\hbar\omega\approx 0.17$ MeV, which is common for low-spin negative-parity structures in this mass region and is interpreted as mixing with octupole vibrational bands [6,26]. Based on the decay pattern observed and a comparison with the $N=93$ neighbor ^{167}W [28] band 2 is tentatively assigned to be the negative-signature, three quasiparticle configuration FAB. However, the cranked Woods-Saxon calculations Fig. 4(a) predict that the EAB configuration is favored at $\hbar\omega>0.2$ MeV, hence a firm assignment awaits further investigation.

It is difficult to assign configurations to the remaining non-yrast states since there are few (if any) γ-ray transitions with which to characterize the nature of these structures. Consequently, the configuration assignments made here are highly speculative. Possible assignments for band 3 include one that is based on the unfavored $\nu i_{13/2}$ $(+,-1/2)$ B orbital or a quasivibrational structure formed by coupling the favored $\nu i_{13/2}$ $(+,+1/2)$ A orbital to a collective phonon excitation.

The $E_x=1978$ keV state, if it is a band head, has an excitation energy in excess of the pair gap and so is likely to be a multi-quasiparticle configuration. Furthermore, the fact that the $E_x=1978$ keV state is located near the midpoint of the excitation energies of the $(27/2^-)$ and $(23/2^-)$ states of band 2 perhaps suggests that it may be the negative-parity signature partner to band 2. This assignment assumes small signature splitting, which is consistent with the predictions of the Woods-Saxon calculations shown in Fig. 4(a). Thus, this state may possibly be assigned as part of the EAB configuration. Further studies of higher-spin states in ^{169}Os are required to eliminate ambiguities associated with the non-yrast configuration assignments.

V. SUMMARY

In summary, excited states have been identified in the neutron-deficient isotope ^{169}Os for the first time using the RDT technique. The bands have been interpreted in terms of quasiparticle excitations within the framework of Woods-Saxon cranking calculations. The onset of the BC quasineutron alignment has been observed and the likely character of this crossing discussed in terms of systematic trends established in the neighboring nuclei. Investigations to higher spins are necessary to quantify the alignment charac-

teristics properly and to eliminate ambiguities associated with the configurations of the non-yrast structures. The establishment of further experimental constraints, such as lifetime measurements, although challenging, would be welcome.

ACKNOWLEDGMENTS

The authors wish to extend their thanks to the crew at the Accelerator Laboratory at the University of Jyväskylä for their excellent technical support. Support for this work was provided by the the UK Engineering and Physical Sciences Research Council (E.P.S.R.C.), the Academy of Finland, the Swedish Natural Science Research Council, and the Access to Large Scale Facility Program under the TMR program of the EU. D.M.C. acknowledges support of Grant No. AF/100225 from the E.P.S.R.C. P.T.G., A.K., and S.L.K. acknowledge financial support from the E.P.S.R.C. P.M.J. and A.K. acknowledge the receipt of Marie Curie Research Training Grants. We also thank the France/UK (IN2P3/EPSRC) Loan Pool for the Eurogam detectors of Jurosphere.

[1] J.L. Wood, K. Heyde, W. Nazarewicz, M. Huyse, and P. Van Duppen, Phys. Rep. **215**, 101 (1992).
[2] J.L. Durell, G.D. Dracoulis, C. Fahlander, and A.P. Byrne, Phys. Lett. **115B**, 367 (1982).
[3] G.D. Dracoulis, R.A. Bark, A.E. Stuchbery, A.P. Byrne, A.M. Baxter, and F. Reiss, Nucl. Phys. **A486**, 414 (1988).
[4] R.A. Bark, G.D. Dracoulis, and A.E. Stuchbery, Nucl. Phys. **A514**, 503 (1990).
[5] P.M. Davidson, G.D. Dracoulis, T. Kibedi, A.P. Byrne, S.S. Anderssen, A.M. Baxter, B. Fabricius, G.J. Lane, and A.E. Stuchbery, Nucl. Phys. **A568**, 90 (1994).
[6] R.A. Bark *et al.*, Nucl. Phys. **A646**, 399 (1999).
[7] D.T. Joss *et al.*, Nucl. Phys. **A689**, 631 (2001).
[8] P.M. Davidson, G.D. Dracoulis, T. Kibedi, A.P. Byrne, S.S. Anderssen, A.M. Baxter, B. Fabricius, G.J. Lane, and A.E. Stuchbery, Nucl. Phys. **A657**, 219 (1999).
[9] B. Cederwall *et al.*, Phys. Lett. B **443**, 69 (1998).
[10] T. Kibedi, G.D. Dracoulis, A.P. Byrne, P.M. Davidson, and S. Kuyucak, Nucl. Phys. **A567**, 183 (1994).
[11] T. Kibedi, G.D. Dracoulis, A.P. Byrne, and P.M. Davidson, Nucl. Phys. **A688**, 669 (2001).
[12] R.S. Simon, K.-H. Schmidt, F.P. Hessberger, S. Hlavac, M. Honusek, H.G. Clerc, U. Gollerthan, and W. Schwab, Z. Phys. A **325**, 197 (1986).
[13] E.S. Paul *et al.*, Phys. Rev. C **51**, 78 (1995).
[14] C.W. Beausang *et al.*, Nucl. Instrum. Methods Phys. Res. A **313**, 37 (1992).
[15] P.J. Nolan, D.W. Gifford, and P.J. Twin, Nucl. Instrum. Methods Phys. Res. A **236**, 95 (1985).
[16] M. Leino *et al.*, Nucl. Instrum. Methods Phys. Res. B **99**, 653 (1995).
[17] M. Leino, Nucl. Instrum. Methods Phys. Res. B **126**, 320 (1997).
[18] C.R. Bingham *et al.*, Phys. Rev. C **54**, R20 (1996).
[19] S.L. King *et al.*, Phys. Lett. B **443**, 82 (1998).
[20] R.D. Page, P.J. Woods, R.A. Cunningham, T. Davinson, N.J. Davis, A.N. James, K. Livingston, P.J. Sellin, and A.C. Shotter, Phys. Rev. C **53**, 660 (1996).
[21] D.C. Radford, Nucl. Instrum. Methods Phys. Res. A **361**, 297 (1995).
[22] C.A. Kalfas *et al.*, Nucl. Phys. **A526**, 205 (1991).
[23] S. Cwiok, J. Dudek, W. Nazarewicz, W. Skalsi, and T. Werner, Comput. Phys. Commun. **46**, 379 (1987).
[24] R. Bengtsson, in *Proceedings of the International Conference on High Spin Physics and Gamma Soft Nuclei, Pittsburgh, 1990*, edited by J.X. Saladin, R.A. Sorensen, and C.M. Vincent (World Scientific, Singapore, 1991), p. 289.
[25] S.M. Harris, Phys. Rev. **138**, B509 (1965).
[26] P. Vogel, Phys. Lett. **60B**, 431 (1976).
[27] J. Kownacki, J.D. Garrett, J.J. Gaardhoje, G.B. Hagemann, B. Herskind, S. Jonsson, N. Roy, H. Ryde, and W. Walus, Nucl. Phys. **A394**, 269 (1983).
[28] K. Theine *et al.*, Nucl. Phys. **A548**, 71 (1992).
[29] M. Neffgen, E.M. Beck, H. Hubel, J.C. Bacelar, M.A. Deleplanque, R.M. Diamond, F.S. Stephens, and J.E. Draper, Z. Phys. A **344**, 235 (1993).